On the discharge processes in pulsed plasma thruster

T. Schönherr[1], M. Stein[2,3], K. Komurasaki[2], G. Herdrich[3]

[1]*The University of Tokyo, Dpt. of Aeronautics and Astronautics, Hongo 7-3-1, 113-8656 Bunkyo, Tokyo, Japan*
[2]*The University of Tokyo, Dpt. of Advanced Energy, Kashiwa-no-ha 5-1-5, 277-8561 Kashiwa, Chiba, Japan*
[3]*University of Stuttgart, Institute of Space Systems, Pfaffenwaldring 29, 70569 Stuttgart, Germany*

This study focuses on the energy conversion processes that yield plasma in a pulsed plasma thruster—one kind of electric space propulsion. High-speed imagery and emission spectroscopy is used to determine the maximum emission during the first few microseconds of the discharge, and an estimation of the temperature distribution is derived. Further, conclusions about the initiation of the discharge are drawn, and compared to similar phenomena used in vacuum insulation. The results show a rapid heating process that concurs with the expected high power-per-mass ratio during the initial phase of the discharge.

1. Introduction

Electric space propulsion uses electric energy to put a propellant into a plasma state and accelerate it by electrothermal, electrostatic, or electromagnetic means. The eventual ejected material yields the thrust to move the spacecraft on which the propulsion system is equipped.

Despite having had their first space flight 50 years ago, the physics involved in pulsed plasma thrusters (PPT) are still too complex to be understood entirely. Especially the differences in resulting plasma behavior between ablative thrusters (solid or liquid) and injection thrusters (liquid or gaseous propellant) cannot be explained with the traditional theory of the early 1960s [1]. In fact, previous research on ablative PPT showed that many assumptions in the theory could not be verified by experiment [2-4], but rather showed similarities to the operation of a vacuum arc thruster (VAT).

Essentially in PPT, stored electrical energy is discharged in an arc, thereby heating, ablating, and ionizing the often-solid propellant, and accelerating the ionized particles by a self-induced magnetic field. Within the short-time PPT discharge, a highly transient, low-temperature, non-equilibrium plasma is formed that was previously studied [3], but the energy conversion from capacitor to plasma and the processes linked with the initiation of the discharge are still hardly investigated.

Using high-speed photography and emission spectroscopy directly in the vicinity of the ablation, this study presents a characterization of the discharge arc and behavior of the involved species. An estimation of the temperature profile in the discharge arc is derived, based on a method by Larenz [5]. Experimental results also helped to understand how the arc is established, although questions remain.

2. Experimental

2.1. Pulsed Plasma Thruster

The PPT used in this study comprises a 80 µF capacitor bank with low inductance and high-current capability, a pair of copper electrodes, solid propellant (PTFE), and a semiconductor spark plug for discharge initiation [6]. Total maximum discharge energy is about 68 J, and an image of the discharge is shown in Figure 1.

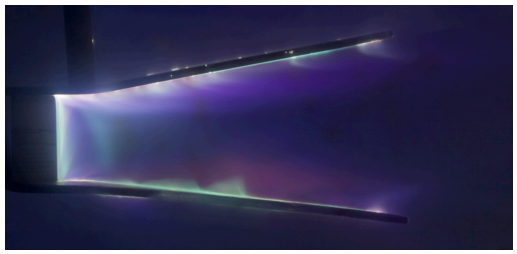

Figure 1: Solid-ablative PPT discharge (up: cathode, down: anode, left: propellant, right: exhaust direction)

2.2. High-speed camera system

For time-dependent studies of the discharge arc position a DRS Hadland Ltd Ultra-8 high-speed camera is used. The camera can record a series of eight 12-bit grayscale pictures with a resolution of 520 x 520 pixels. A Nikon 105 mm f/2.8 lens is applied to focus on the PPT and to for adjustment of aperture. Several bandpass filters (D = 20 mm) are placed – one at a time – between camera and vacuum chamber window. Filters are used according to known spectral emission lines of all relevant species and their intensity, based on spectroscopic studies of the plasma bulk [3]. For practical reasons and availability of filters the relevant lines were limited to F II, F III, C_2, C II, C III, C IV and Cu II.

2.3. Optical emission spectroscopy system

In this work a SOL instruments MS3504i spectrometer is used together with an Andor Technology iStar DH734-18F-03 iCCD camera.

The spectrometer has a spectral resolution of 0.12 nm and covers a range of 30 nm. The central wavelength of this range can be moved anywhere between 330 and 1000 nm.

The iCCD camera has an image resolution of 1024 x 1024 pixels and is capable of exposure times down to 2 ns.

3. Temperature estimation

Based on the work by Larenz [5], it is known that each spectral line emits at maximum intensity at a characteristic pressure-dependent temperature. For atoms and ions, this temperature *T'* can be calculated by solving:

$$\frac{h^3}{(2\pi m)^{3/2}} \cdot \frac{1}{2} \cdot \frac{g_i}{g_k} \cdot \frac{p}{E_{ion}^{5/2}} \cdot \left(\frac{E_{ion}}{kT'}\right)^{5/2} \cdot \exp^{\frac{E_{ion}}{kT'}} = \left(\frac{\frac{E_{ion}}{kT'} + \frac{5}{2}}{\frac{E_k}{kT'} - 1}\right)^2 - 1$$

For exemplary expected spectral lines of PTFE plasma, the temperature-dependent emission at $p = 1$ bar is plotted in Figure 2, and the calculated characteristic temperatures T' are listed in Table 1.

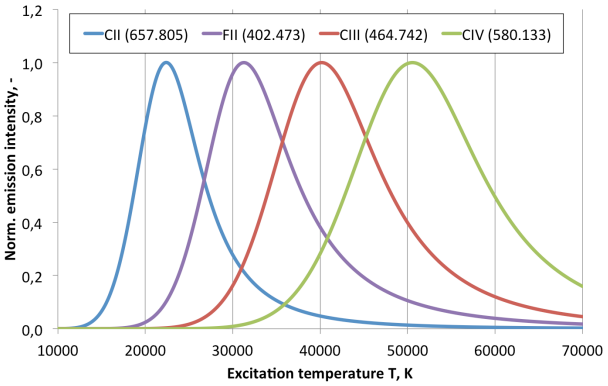

Figure 2: Exemplary temperature-dependent normalized spectral emission intensity for PTFE plasma species (wavelengths in brackets; in nm)

Table 1: Calculated characteristic temperatures

Species (λ in nm)	Characteristic temperature
CII (657.805)	22395 K
F II (402.473)	31278 K
C III (464.742)	40171 K
C IV (580.133)	50554 K

During the PPT discharge, one can expect a pressure inside the bulk plasma of less than 1 bar, but higher than 0.1 bar [3]. Calculating the characteristic temperature for the pressure range for all spectral lines expected to be emitted by the plasma in the observed range, one obtains Figure 3.

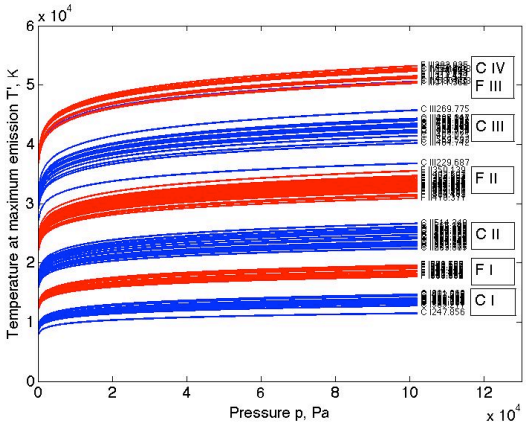

Figure 3: Pressure dependency of T' for observable species in PTFE plasma

The data show that the error caused by the uncertainty of the plasma pressure is small. Further, the relations between the species do hardly change over the pressure range, which means that a discussion of the temperature distribution is still valid even if an uncertainty on the absolute temperature value exists.

4. Results and Discussion

4.1. Arc position and width

The discharge characteristics of the PPT (discharge current, discharge voltage, voltage of spark plug) are plotted in Figure 4, and exemplary full-VIS-range images taken by the high-speed camera are in Figure 5.

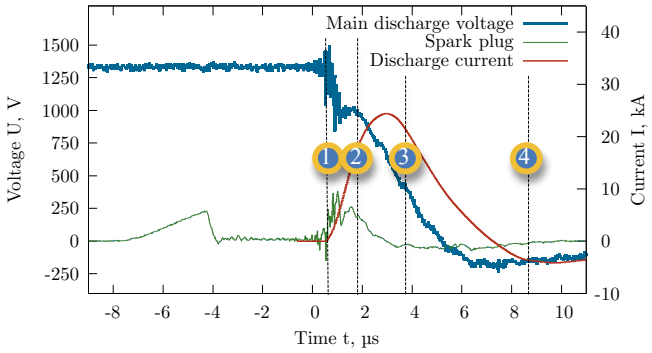

Figure 4: Discharge characteristics

As can be seen, a strong emission in shape of an arc forms between the electrodes and remains stable for the main part of the electric power throughput. As the current fades (between points 3 and 4), the arc destabilizes and becomes diffuse.

As emission from many species is expected, the full-VIS observation only represents a convolution of all emissions caused by electronic excitation. To gain information on individual species, bandpass filters are applied, and the images processed to

determine the position of maximum emission plotted in Figures 6.

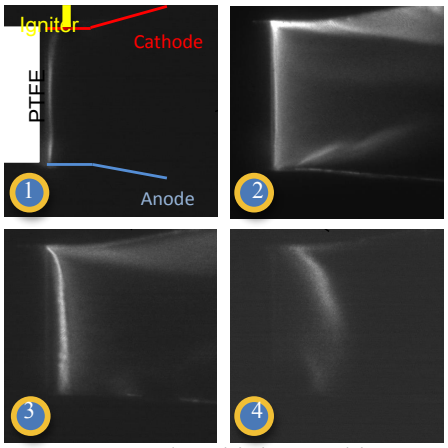

Figure 5: Exemplary high-speed images of breakdown and plasma movement

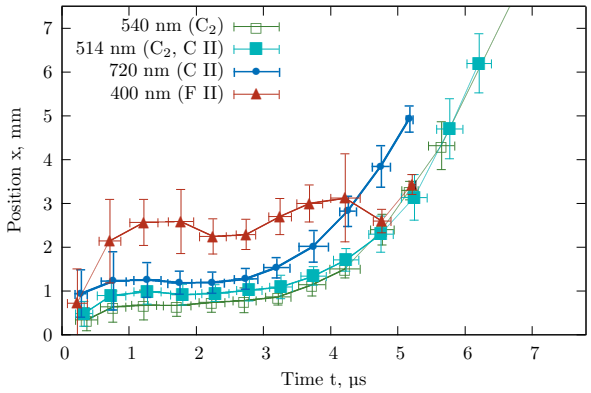

Figure 6: Position of emission maxima for different bandpass filters (center wavelength and pertinent species marked)

The data show that the emission maxima remain almost at constant position for each species for the first 4 µs, whereas all maxima move downstream as the current drops. Given that the current shows a strong gradient and powers the ablation of the propellant, one would expect that the maxima shift depending on the temperature changes, but the results indicate that a balance is found between ablation and heating as the current increases.

4.2. Temperature distribution

For estimation of the temperature in the discharge chamber, emission data were taken along the normal of the propellant surface. Emission maxima for each spectral line were calculated and show consistent information with Figure 6. Using the characteristic temperature data for 1 bar from Figure 3, one can link each point with a temperature. This works only for atoms and ions. The C_2 molecule is quite dominant in the spectra, and would yield valuable information for the temperature distribution, but an estimation of temperature does require a numerical radiation modeling beyond the scope of this paper. This study assumes the emission temperature to be 5000 K, knowing that this is a very rough guess. Further, the propellant surface is considered to be about 1100 K, which was found previously as the typical surface temperature during ablation of PTFE. Combining all these data yields Figure 7 that shows the temperature distribution during the discharge.

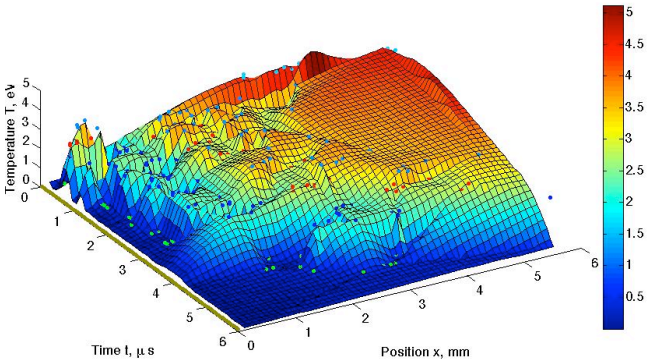

Figure 7: Temperature distribution in the PPT discharge (blue points: C II [dark] to C IV [cyan], red: F II, green: C_2, yellow: surface temperature)

Temperatures of up to 5 eV are reached, higher than the 3.5 eV measured in the plume beyond 10 mm, indicating a energy dissipation. A strong gradient in the temperature is observed especially during the initial microsecond. Given the high instantaneous power of the PPT discharge and the small mass (few µg) ablated during the entire discharge, one can suspect that the power-to-mass ratio is extremely high during this initial stage resulting in high ionization and strong heating of the propellant. As the discharge continues, the temperature decreases, despite the current increasing, indicating that the ratio becomes smaller. It is to be noted that the particles are expected to be accelerated to up to 40 km/s in the few mm from the propellant surface, so the emission data might be convoluted with a velocity field of the particles.

4.3. Discharge initiation

From previous research, it is known that the ablation of the PTFE propellant is a continuous process throughout the discharge that follows the power input onto the surface. Radiation and particle flux were suspected to be the main energy input. However, as heating of the PTFE surface requires a certain time before material is ablated, the ablation is not concurrent with the breakdown in the simulation. The high-speed images and the spectroscopy, however, show an immediate presence of material in

the inter-electrode space after breakdown happens. From Figure 5-1, one sees that the arc is slightly bent towards the ignited on the cathode side after the breakdown indicating that a conducting connection was first established there, before the arc finds the lower resistance of the main cathode. This would also explain the increase in spark plug voltage after main breakdown. With Figure 4, it is clear that some time passes between the discharge of the spark plug, and the main breakdown possibly with material being ablated in this time already before main breakdown. From the theory of vacuum insulation [7], it is known that breakdown occurs when primary electrons formed at the triple junction point (cathode – insulator – vacuum) hit the insulator surface and yield secondary electron emission and electron-stimulated desorption eventually leading to an avalanche flashover. Given that the primary electrons in the PPT discharge are firstly introduced by the spark plug discharge, one can speculate that electron-stimulated desorption happens in the few μs preceding the breakdown, and, thus, facilitate the ablation of the propellant when the breakdown occurs. This hypothesis is, however, yet to be verified by experiment.

5. Conclusions

The temperature profile in a PPT discharge plasma was estimated for the first time, and shows that the heating of the propellant occurs at a very steep rate at the initial phase during the current rise, whereas the maximum current does not yield the maximum temperature.

Pre-breakdown phenomena are indicated by the experimental data regarding desorption of propellant material by electron impact from the spark plug that facilitate the ablation in the main discharge.

6. References

[1] R. Jahn, *Physics of Electric Propulsion*, McGraw-Hill Book Company, New York, NY, USA, 1968

[2] M. Lau et al., "Investigation of the Plasma Current Density of a Pulsed Plasma Thruster", *J. Prop. Power,* **30** (2014) 1459.

[3] T. Schönherr et al., "Characteristics of plasma properties in an ablative pulsed plasma thruster", *Phys. Plasmas*, **20** (2013) 033503.

[4] M. Keidar et al., "Ionization and ablation phenomena in an ablative plasma accelerator", *J. Appl. Phys.*, **96** (2004) 5420.

[5] R. W. Larenz, "Über ein Verfahren zur Messung sehr hoher Temperaturen in nahezu durchlässigen Bogensäulen," *Zeit. f. Phys.*, **129** (1951) 327.

[6] T. Schönherr et al., "Propellant utilization efficiency in a pulsed plasma thruster", *J. Prop. Power,* **29** (2013) 1478.

[7] R. V. Latham, *High Voltage Vacuum Insulation: The Physical Basis*, Academic Press, Inc, London, UK, 1981